Proceedings of the INMM & ESARDA Joint Virtual Annual Meeting
August 23-26 & August 30-September 1, 2021

ORGANIC GLASS SCINTILLATOR CHARACTERIZATION FOR RADIOXENON DETECTION

L. M. Clark[1*], T. E. Maurer[1], N. Giha[1], S. D. Clarke[1], S. A. Pozzi[1]
[1]*Nuclear Engineering and Radiological Sciences, University of Michigan, Ann Arbor, 48109*
[*]*email: clarklea@umich.edu*

Abstract
The International Monitoring System utilizes four areas of detection for above and below ground explosions. Nuclear events can be confirmed through detection of radioxenon isotopes ^{131m}Xe, ^{133}Xe, ^{133m}Xe, and ^{135}Xe from atmospheric samples. Beta-gamma coincidence detection systems that utilize plastic scintillators for beta particle detection and sodium iodide for correlated gamma ray detection are used to identify these isotopes. However, plastic scintillators exhibit memory effects and poorer energy resolution compared to other materials. Past investigations into stilbene as a viable alternative to plastic for this application saw reduced memory effect but comparable energy resolutions. Construction of stilbene scintillators was found to be difficult due to its fragile material, as well. Organic glass scintillators are of interest because the glass demonstrates similar properties to stilbene, high light output, and is easier to construct. In this work, custom molds were used to cast the glass into desired shapes, providing a wide array of research options. Pulse shape discrimination capabilities and light collection were investigated using different thicknesses and reflector wrappings of organic glass scintillators. These results will be used as groundwork in the development of an organic glass beta detector, similar to the plastic scintillators deployed in the field.

Introduction
Efforts towards nuclear nonproliferation have existed since the creation of the first nuclear weapon [1]. Several international treaties were implemented to support these efforts over many decades, including the Comprehensive Nuclear-Test-Ban Treaty (CTBT) of 1996. This treaty prohibits all nuclear explosions, including testing, in the atmosphere, underwater, and underground. Part of the verification regime to enforce compliance includes the International Monitoring System (IMS), which uses four detection technologies: seismic, hydroacoustic, infrared, and radionuclide. While the first three areas are used to identify if an event has occurred, either natural or anthropogenic, radionuclide detection verifies if the event was nuclear. For underground testing purposes, this involves studying the prominence of specific radioactive xenon, or radioxenon, isotopes: ^{131m}Xe, ^{133}Xe, ^{133m}Xe, and ^{135}Xe. These four isotopes were chosen because they have the highest cumulative fission yield of the noble gas fission products in uranium and plutonium; the isotopes also have long enough half-lives to be measured and analyzed in a timely manner, but not too long to where the signatures could be mistaken with background radiation [2,3]. This information is shown in Table 1.

Table 1. Half-lives and cumulative fission yields for ^{235}U and ^{239}Pu induced by thermal neutrons for the isotopes of interest [3].

Isotope	**Half-Life**	**Fission Yield ^{235}U**	**Fission Yield ^{239}Pu**
^{135}Xe	9.1 hours	6.61%	7.36%
^{133}Xe	5.24 days	6.6%	6.99%
^{133m}Xe	2.19 days	0.189%	0.216%
^{131m}Xe	11.9 days	0.0313%	0.041%

Typical detection systems used in radionuclide monitoring use beta-gamma coincidence measurements with plastic scintillators for beta particle detection and inorganic scintillators, such as NaI(Tl), for gamma detection [4-6]. Atmospheric samples are collected continuously around the world and measured for radioxenon signatures. One drawback to this approach is the so-called "memory effect" that remains after the sample containing xenon diffuses into the plastic beta cell scintillator. This remaining activity increases the background for future measurements and increases the minimum detectable amount (MDA) of the system [7]. Past investigations for improving these detection systems have included research into different scintillation materials to replace plastic beta cells. For example, stilbene organic scintillators have been shown to have reduced memory effect compared to plastic but similar energy resolution [8]; however, stilbene has a high cost of production and is brittle. Our group has begun characterizing organic glass scintillating material (OGS) as a potential detector for radionuclide monitoring because it has similar properties to stilbene, including pulse shape discrimination (PSD) and high light output, and it is easier to construct [9].

Here, we study the effects that different OGS configurations have for light collection, PSD, and detector efficiencies. Configurations include using diffuse and retroreflective wrappings and varying OGS detector thicknesses. Along with the primary goal of research towards OGS characterization, these results will be considered in future work for an OGS beta cell, similar to the plastic cell deployed in the field. This beta cell needs to be thin enough to allow gamma rays to escape and be detected with gamma detectors, but thick enough to detect the beta particles from the radioxenon. Further characterization requires time and energy resolution investigations before the beta detector development.

Description of the Work

Organic Glass Scintillator

Scientists at Sandia National Laboratories developed the OGS, and it has quickly become an interest in nuclear nonproliferation efforts due to its PSD capability, high light output, and fast emission characteristics [9,10]. OGS is easily moldable because it is amorphous; therefore, melt-casting techniques can be employed to cast the scintillator into any shape desired. These known advantages make OGS detectors an appealing choice for radionuclide monitoring.

Our laboratory at University of Michigan is equipped to melt-cast our own OGS detectors. First, a silicone mold is prepared into the desired shape of the detector. For this investigation, 12.7 × 25.4

mm rectangular “slabs” with thicknesses 2, 3, 4, and 5 mm were studied and prepared using molds to fit these dimensions. Slab dimensions were used to mimic an unfolded plastic beta detector cell seen in the field. Previous work has shown that pre-heating the mold and slowly cooling the melt to room temperature prevented detrimental internal stress [9]. Therefore, the mold was preheated in an oven set at 130 °C prior to the glass pouring. For the melt-casting procedure, the OGS material is placed in a vial and warmed to 200 °C using a hot plate and heat gun. Simultaneously to the heating process, the vial is attached to a vacuum pump to remove any dissolved air and prevent bubbles. Once the material has melted, the vial is removed from the vacuum/heating system and quickly poured into the mold. The melt is set in the oven for 14 hours of cooling; once the process is complete, the glass is carefully removed from the mold and ready to be used in experiments.

Experimental Procedures

To study the effects of reflective wrappings and slab thickness on OGS detectors, several experiments with gamma and neutron sources were conducted. Common reflectors, such as Lambertian (diffuse) and retroreflective, are used to maximize light collection in scintillator-based detectors [11]. The three reflective studies, shown in Figure 1, include white Teflon tape acting as a diffuse reflector, 3M Scotchlite™ Silver Reflective Tape as the retroreflective wrapping, and a case with no reflective wrapping. In total, there were twelve different detectors studied in this work. Each slab was carefully wrapped in the respective material, or left unwrapped, and optically coupled with a Selvol 09-425 polyvinyl alcohol solution to a 7.62 cm diameter photomultiplier tube (PMT), as shown in Figure 2. The assembly was placed in a custom dark box. High voltage and digitizer cables were connected to the system through bulkheads drilled into the dark box and covered with black tape and a black tarp. The cables fed into the voltage supply set at 1650 V and a CAEN Technologies DT5730 digitizer.

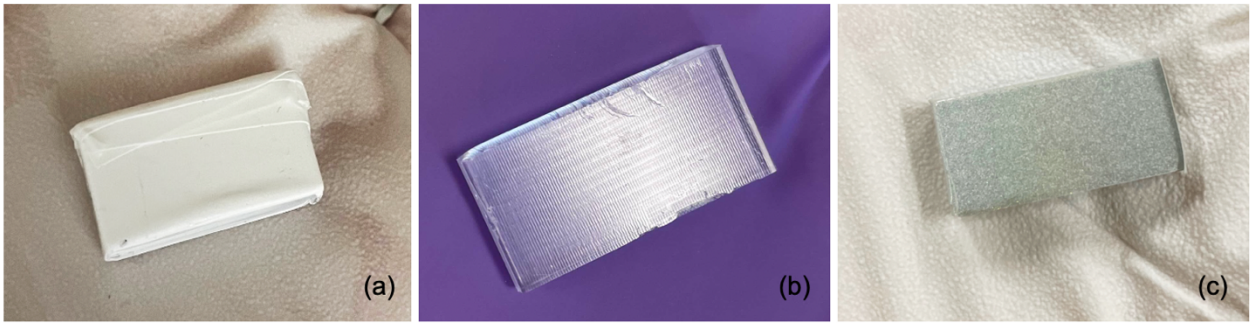

Figure 1: OGS slabs measuring 12.7 × 25.4 × 3 mm with (a) diffuse, (b) no wrapping (bare), and (c) retroreflective wrappings.

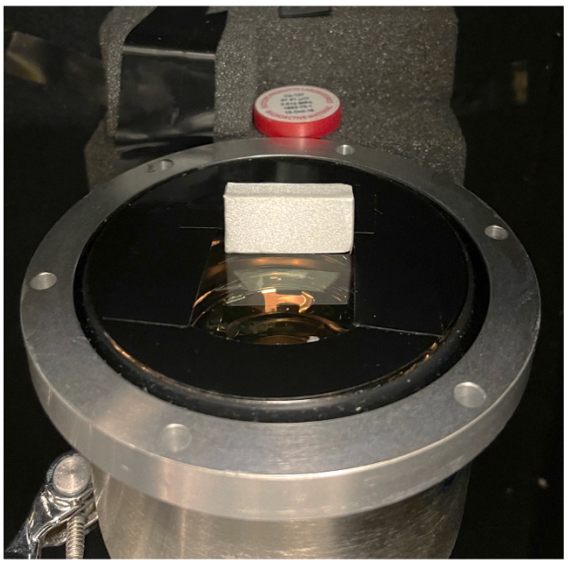

Figure 2: Example retroreflective OGS slab optically coupled to a 7.62 cm diameter PMT with a ^{137}Cs source placed in line with detector. The setup is placed inside the dark box for light-tightness.

Table 2 contains a description of the radiation sources used in this work. The ^{137}Cs source was used for the energy calibration of each detector along with gamma spectroscopy. This source was placed directly inside the dark box 6.25 cm from the OGS slab, as shown in Figure 2, for all of its measurements. Bare, diffuse, and retroreflected OGS slabs of thicknesses 2, 3, 4, and 5 mm were tested with this source. The ^{252}Cf and ^{239}PuBe sources were used to study the PSD capabilities of the glass. The ^{252}Cf source was placed 33 cm away from the OGS slab outside of the dark box. Due to available resources at the time, only the bare and diffuse-wrapped OGS slabs were tested with this source. The ^{239}PuBe source was also placed 33 cm away from the OGS slab outside of the dark box. Two measurements with this source were performed with the most extreme OGS cases: the 5 mm diffuse-wrapped slab and the 2 mm bare slab.

Table 2. Measurement times and activities of the three sources used in this work.

Source	**Meas. Time (min)**	**Activity (μCi)**
^{137}Cs	5	77.57
^{252}Cf	5	1182.45
^{239}PuBe	120	998,340.96

Results & Discussion

The ^{137}Cs calibration measurements were used to convert arbitrary units of the digitizer into light collection in units of mega electron-volts, electron equivalent (MeVee), which is equal to the amount of light produced by a recoil electron of the corresponding energy [12]. The dominant interaction for organic scintillators of low atomic number materials, such as OGS, is Compton scattering [13]. Therefore, the 478 keV Compton edge for ^{137}Cs was used as our calibration point. Figure 3(a) shows the pulse height corresponding to the Compton edge for the twelve OGS slab configurations. A

higher Compton edge position indicates higher light collection: the diffuse-wrapped slabs produce a higher light collection than the bare and retroreflective cases. Figure 3(b) shows the full ^{137}Cs pulse height spectra to better visualize the light collection from different slab configurations of the same thickness, 4 mm. The diffuse-wrapped spectra extend to larger pulse height values, with retroreflective and bare following.

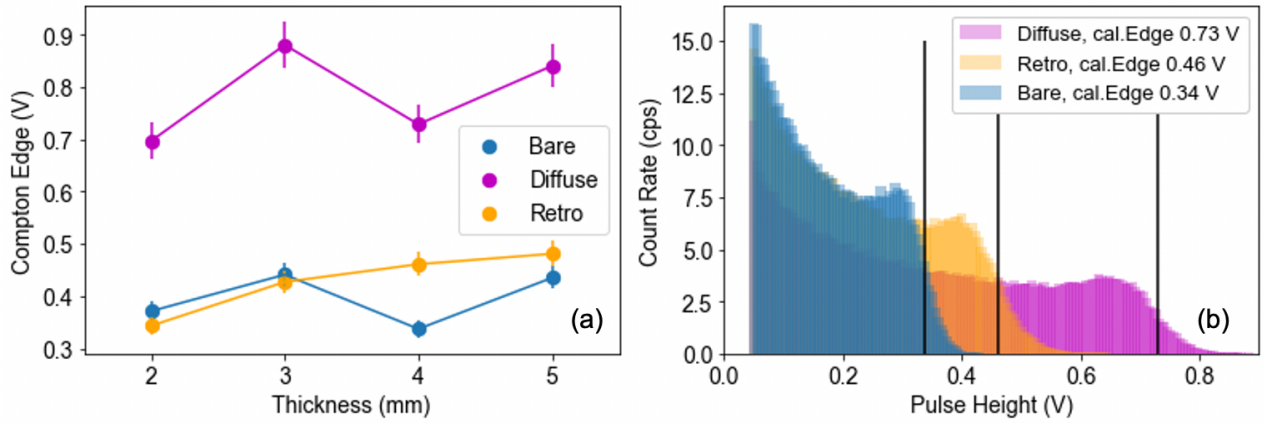

Figure 3: (a) Comparison of ^{137}Cs Compton edge values as a function of thickness for bare, diffuse, and retroreflective-wrapped OGS slabs; (b) An example ^{137}Cs pulse height spectrum using an OGS slab with a 4 mm thickness. The overlapping spectra indicate the reflective wrappings used with a protruding line taken at 50% of the Compton edge for energy calibration.

Figure 4 shows the pulse height spectra in MeVee obtained with the ^{137}Cs source for 3 mm bare, diffuse, and retroreflected wrapped slabs. The box highlights an isolated Compton edge region from 0.4 – 0.66 MeVee. This region is isolated specifically because it represents the gamma rays that roughly deposit their maximum energy into the detector (0.662 MeV, with a detected 0.478 MeV recoil electron). The slopes of the spectra differ from one another, with the diffuse-wrapped OGS having the steepest; this is a possible indication into energy resolution information from the various reflective wrappings. Energy resolution refers to a detector's ability to accurately identify the energy distribution of incoming radiation [13]. A wider distribution (slope) may indicate more fluctuations recorded from pulse to pulse even though the incident energy deposited into the detector remains the same. Energy resolution is an important component of detector characterization and will be investigated in future work for this material.

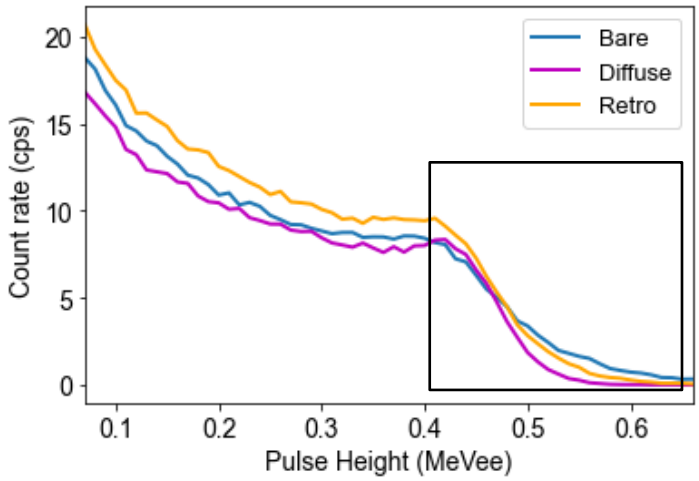

Figure 4: An example ^{137}Cs pulse height spectrum with count rates using a 3 mm thick OGS slab and various reflective wrappings.

PSD techniques are used to discriminate neutron events and gamma ray events in in a single detector. These techniques have many applications in nuclear physics and nuclear nonproliferation and are often used with organic scintillators, such as liquid or stilbene [12,14,15]. The PSD capabilities of the OGS slabs were explored using ^{252}Cf and ^{239}PuBe sources. We implemented a charge integration technique with the tail integral of the pulses starting 10 ns after the maximum pulse height and total integration length of 400 ns. The pulse integrals were converted from V-ns to MeVee using the ^{137}Cs calibration. Figure 5 shows an example PSD scatterplot with tail-to-total ratios and pulse integrals up to 0.7 MeVee using the 5 mm diffuse-wrapped OGS slab. The total counts from this measurement, both neutrons and gamma rays, is 280,714. Using all the data above the discrimination line to represent the neutron counts, a total of 95,020 neutron counts were recorded for this measurement.

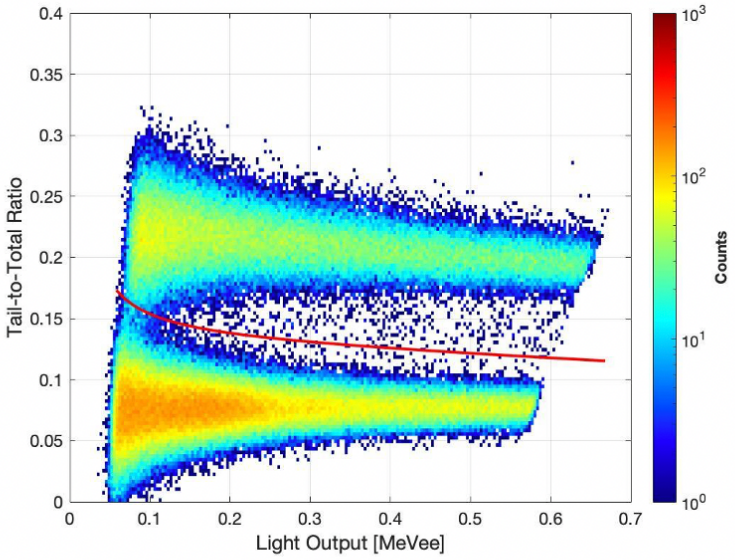

Figure 5: PSD scatterplot with tail-to-total ratios against light output for ^{239}PuBe using a 5 mm thick, diffuse-wrapped OGS slab. A line of discrimination in red is an estimate for classifying neutrons (above line) and gamma rays (below).

Detector efficiency is the measure of the radiation percentage detected from the overall yield emitted by a source [16]. Absolute efficiency is the ratio of the number of counts recorded to the radiation quanta emitted by the source; intrinsic efficiency is the ratio of the number of pulses recorded to the number of radiation quanta incident on the detector. Because the orientation and distance of the source to slab remained approximately the same, the minimal change in absolute efficiency is not substantial in this work. However, the intrinsic efficiency does change with detector thickness, and therefore, the detector efficiency may be enhanced by increasing the thickness, as generally seen in Figure 5.

Figure 6(a) shows the intrinsic efficiencies measured with ^{137}Cs using twelve different OGS configurations of varying thickness and reflective wrapping. Figure 6(b) provides the neutron efficiencies for light output ranges from 0.05 – 0.7 MeVee measured with ^{252}Cf with eight different OGS slabs. The neutron counts were obtained using PSD techniques like those seen with the ^{239}PuBe in Figure 5, where the number of neutrons equal the total counts above the discrimination line. The retroreflective wrapping used in the ^{137}Cs measurements was not available at the time the ^{252}Cf measurements were performed. In general, we see a positive correlation between efficiency and thickness: as the thickness of the OGS increases, as do the efficiencies. The diffuse-wrapped slab produced higher efficiencies for each thickness compared to the bare case. This is expected behavior seen in diffuse reflectors as they minimize the amount of escaped light [11].

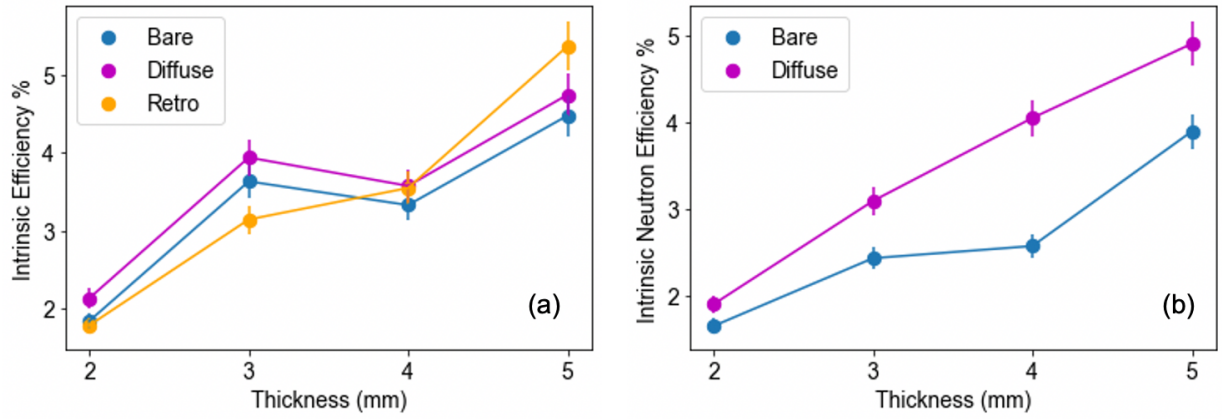

Figure 6: (a) Intrinsic efficiencies for bare, diffuse, and retroreflective wrappings as a function of OGS slab thickness measured using a ^{137}Cs source; (b) Intrinsic neutron efficiencies for bare and diffuse wrappings as a function of thickness measured using a ^{252}Cf source.

Conclusion

In this work, we investigated the effects that thickness and added reflectors have on OGS detectors when detecting gamma and neutron sources. We observe higher pulse heights, thus better light collection, in diffuse-wrapped OGS slabs compared to the retroreflected or unwrapped slabs. We see a steeper slope in the isolated ^{137}Cs Compton edge region in the diffuse-wrapped OGS slab pulse height spectra compared to bare and retroreflective. With this information, combined with the light collection results, we can expect to see better energy resolution in configurations with diffuse wrappings. Further work on energy resolution is needed to confirm this observation. We observed

the PSD capabilities of the OGS material and plan to continue with different neutron sources and slab configurations. In general, we also see a positive correlation between thickness and intrinsic efficiency for both neutrons and gammas. These results show that OGS detectors have the potential to compete with leading organic scintillators and make improvements in radioxenon monitoring and nuclear nonproliferation efforts. Further characterization, such as time and energy resolution, is necessary before radioxenon measurements and OGS beta cell development can begin.

Acknowledgements
This work was funded in-part by the Consortium for Monitoring, Technology, and Verification under Department of Energy National Nuclear Security Administration award number DE-NA0003920. The authors would like to thank Dr. Lucas Nguyen of Sandia National Laboratories and Dr. Christine Johnson of Pacific Northwest National Laboratory for their insight and help to this work.

References

1. CTBTO 2010. *History: Summary*. History: Summary: CTBTO Preparatory Commission. [Online]. Available: https://www.ctbto.org/the-treaty/history-summary/
2. P. E. Keller, (2012, April). *Categorization of Radioxenon* . Pacific Northwest National Laboratory. https://www.pnnl.gov/main/publications/external/technical_reports/PNNL-21331.pdf.
3. C. B. Sivels, (2018). Development of an Advanced Radioxenon Detector for Nuclear Explosion Monitoring (Handle: 2027.42/147543) [Doctoral dissertation, University of Michigan, Ann Arbor]. Deep Blue
4. A Ringbom, *et al.,* "SAUNA—a system for automatic sampling, processing, and analysis of radioactive xenon," *Nuclear Instruments and Methods in Physics Research Section A: Accelerators, Spectrometers, Detectors and Associated Equipment,* vol. 508, pp. 542-553, 2003 https://doi.org/10.1016/S0168-9002(03)01657-7.
5. J. I. McIntyre, *et al., "*Measurements of ambient radioxenon levels using the automated radioxenon sampler/analyzer (ARSA)." *Journal of Radioanalytical and Nuclear Chemistry* 248, 629–635 (2001). https://doi.org/10.1023/A:1010672107749
6. V. V. Prelovskii, *et al.* The ARIX-03F mobile semiautomatic facility for measuring low concentrations of radioactive xenon isotopes in air and subsoil gas. *Instrum Exp Tech***,** 393–397 (2007). https://doi.org/10.1134/S0020441207030165
7. L. Blackberg, *et al.,* "Investigations of surface coatings to reduce memory effect in plastic scintillator detectors used for radioxenon detection," *Nuclear Instruments & Methods in Physics Research Section A: Accelerators, Spectrometers, Detectors and Associated Equipment*, vol. 656, no. 1, pp. 84 – 91, 2011. [Online]. Available: http://www.sciencedirect.com/science/article/pii/S0168900211014884
8. C. B. Sivels, *et al.* "Stilbene cell development to improve radioxenon detection", *Nuclear Instruments and Methods in Physics Research Section A: Accelerators, Spectrometers, Detectors and Associated Equipment,* vol. 923, pp.72-78, 2019 https://doi.org/10.1016/j.nima.2019.01.022
9. Feng P.L., Myllenbeck N.R., Carlson J.S. (2021) Organic Glass Scintillators. In: Hamel M. (eds) Plastic Scintillators. Topics in Applied Physics, vol 140. Springer, Cham. https://doi.org/10.1007/978-3-030-73488-6_8

10. J. S. Carlson, P. Marleau, R. A. Zarkesh, and P. L. Feng. “Taking Advantage of Disorder: Small-Molecule Organic Glasses for Radiation Detection and Particle Discrimination.” United States: N. p., 2017. Web. https://doi.org/10.1021/jacs.7b03989
11. M. Folsom, P.A. Hausladen, J.P. Hayward, J. Nattress, K.P. Ziock, “Characterization of retroreflective tape optical properties for use with position-sensitive scintillator detectors,” *Nuclear Instruments and Methods in Physics Research Section A: Accelerators, Spectrometers, Detectors and Associated Equipment,* vol. 1005, 2021 https://doi.org/10.1016/j.nima.2021.165365
12. M. Flaska, S. A. Pozzi, “Identification of shielded neutron sources with the liquid scintillator BC-501A using a digital pulse shape discrimination method,” *Nuclear Instruments and Methods in Physics Research Section A: Accelerators, Spectrometers, Detectors and Associated Equipment,* vol.577, pp. 654-663, 2007 https://doi.org/10.1016/j.nima.2007.04.141
13. G. F. Knoll, *Radiation detection and measurement; 4th ed.* New York, NY: Wiley, 2010.
14. M. L. Ruch, M. Flaska, and S. A. Pozzi. “Pulse shape discrimination performance of stilbene coupled to low-noise silicon photomultipliers.” United States: N. p., 2015. Web. doi:10.1016/j.nima.2015.04.053.
15. T. A. Laplace, et al., “Comparative scintillation performance of EJ-309, EJ-276, and a novel organic glass” JINST, vol. 15, 2020, doi.org/10.1088/1748-0221/15/11/p11020
16. I. Akkurt, K. Gunoglu, S. S. Arda, "Detection Efficiency of NaI(Tl) Detector in 511–1332 keV Energy Range", *Science and Technology of Nuclear Installations*, vol. 2014, Article ID 186798, 5 pages, 2014. https://doi.org/10.1155/2014/186798